Accepted for publication by IEEE Transactions on Smart Grid (DOI: 10.1109/TSG.2020.3020790)



# Real-Time Area Angle Monitoring using Synchrophasors: A Practical Framework and Utility Deployment

Wenyun Ju, *Member*, *IEEE*, Ian Dobson, Kenneth Martin, *Fellow*, *IEEE*, Kai Sun, *Senior Member*, *IEEE*, Neeraj Nayak, Iknoor Singh, Horacio Silva-Saravia, Anthony Faris, Lin Zhang, Yajun Wang, *Member*, *IEEE*

***Abstract*—This paper develops a practical framework of Area Angle Monitoring to monitor in real time the stress of bulk power transfer across an area of a power transmission system. Area angle is calculated from synchrophasor measurements in real time to provide alert to system operators if the area angle exceeds pre-defined thresholds. This paper proposes a general method to identify the warning threshold of area angle and a simplified method to quickly update area angle thresholds under significant topology change. A mitigation strategy to relieve the area stress is also proposed. In order to handle the limited coverage of synchrophasor measurements, this paper proposes a method to estimate phase angles for boundary buses without synchrophasor measurements, which extends the application scenario of AAM. AAM is verified for a power transmission area in the Western Electricity Coordinating Council system with both simulated data and synchrophasor measurements recorded from real events. A utility deployment for real-time application of AAM with livestream and recorded synchrophasor data is described.**

***Index Terms*—Real-time application, area angle, synchrophasor measurements, wide area monitoring, mitigation strategy**

## I. Introduction

THE stress of bulk power transfer through an area suddenly increases when there are multiple line outages inside the area. Therefore it is important to monitor the stress in real-time and provide an alert to system operators if the outages cause overloads that make the system insecure. Then appropriate control actions can be taken to relieve the stress.

Synchrophasor technology is developing rapidly in recent years. Synchrophasor technology uses monitoring devices, called phasor measurement units, which take high-speed measurements of phase angles, voltage and frequency that are time stamped with high-precision clocks. The measurements, typically taken 30 times a second, can quickly track system changes undetectable through traditional monitoring systems used in the industry [1]. This makes new energy management applications possible, including model validation [2], dynamic state estimation [3], oscillation monitoring, islanding detection and wide area monitoring.

References [4], [5] use angle difference between two buses to monitor the stress of power flow. Phase angle difference is primarily driven by power flow and electrical impedance. And a large phase angle difference between the source and the sink or a pair of buses indicates greater power flow between those points [6].

Not only detecting the stress of power flow is important, but also relieving the stress is critical. Simulations of the system state before the 2003 USA/Canada blackout suggest the importance of increased angle difference for triggering blackouts [4]. Indeed, many large cascading outages start with multiple outages initially occurring at a slow rate due to line overloads and other effects [7]–[11]. Some cascading outages could be prevented if there are methods giving the situational awareness for fast emergency actions to relieve stress caused by multiple outages [12]–[14]. The need for fast emergency actions can also arise when there are multiple simultaneous outages during extreme events such as storm, fire, icing, or an earthquake.

The angle difference between two buses can detect a general stress but does not associate that stress to particular patterns of power flow. Therefore the angle difference between two buses is not associated with an action to mitigate the stress and it is hard to define thresholds for the angle between two buses.

Although there are some established methods of detecting and resolving overloads due to power transfers. References [15]–[17] compute minimum security margins under operational uncertainty with respect to thermal overloads. Reference [18] provides a tool for computation of transfer capability margins. These methods and applications are developed on top of SCADA and state estimation at the SCADA sampling rate.

Area angle [19]–[21] uses angle difference for an area to track the bulk power stress due to line outages inside the area using synchrophasor measurements, it is approximate but faster when compared with SCADA and state estimation. Meanwhile, area angle is associated with a particular pattern of power flow through the area, which allows thresholds for area to be set up. Moreover, mitigation is most essential under emergency conditions of multiple outages, and this is when the state estimation is most likely to fail and area angle using synchrophasor measurements is most necessary. Since

This work was supported by DOE under Award Number DE-OE0000849.

W. Ju, K. Martin, N. Nayak, I. Singh, and H. Silva-Saravia are with Electric Power Group, LLC, Pasadena, CA USA (e-mail:wenyunju@gmail.com).

I. Dobson is with Iowa State University, Ames, IA USA (e-mail:dobson@iastate.edu).

K. Sun is with University of Tennessee, Knoxville, TN USA (e-mail:kaisun@utk.edu).

A. Faris is with Bonneville Power Administration, Vancouver, WA USA (e-mail:ajfaris@bpa.gov).

L. Zhang is with American Electric Power, New Albany, OH USA (e-mail:lin.zhang.ece@gmail.com).

Y. Wang is with Dominion Energy, Richmond, VA USA (e-mail:yajun.wang@dominionenergy.com).

reducing the area bulk power transfer can be translated into a specific action, the area angle is not only monitoring but also supplying actionable information to mitigate the stress. Thus area angle can realize real-time monitoring and mitigation of area stress.

As a summary, Area Angle Monitoring (AAM) uses synchrophasor measurements to calculate area angle to monitor the specific stress of bulk power transfer across an area caused by different outages within the area in real time and perform mitigation if needed. The concept of area angle is proposed in [19], [20] based on circuit theory. Reference [21] shows that the area angle tracks the bulk power stress due to line outages inside the area and gives alarm/warning and emergency thresholds of area angle.

The final objective of AAM is to practically apply AAM in real-time using synchrophasor measurements. Currently, area angle is not a mature technology. It requires many efforts to be further developed. The main challenges are:

1) A practical framework of AAM for real-time monitoring of bulk power transfer stress is needed to guide utilities to apply AAM within their footprints.

2) AAM requires synchrophasor measurements for all the boundary buses of the monitored area in order to calculate area angle. However, in reality, some boundary buses may not have synchrophasors.

3) The methods for quickly calculating area angle thresholds need development.

4) The deployment of AAM and testing using synchrophasor measurements in utilities needs to be done.

5) Mitigation strategies to reduce the area bulk power transfer need investigation.

This paper addresses these challenges and moves AAM towards industry application. The main contributions are:

1) A practical framework of AAM for real-time monitoring of bulk power transfer stress is proposed, which can guide utilities to apply AAM within their footprints. A real-time monitoring platform of AAM is developed and deployed at Bonneville Power Administration (BPA).

2) Phase Angle Compensation (PAC) is proposed to support the calculation of area angle when not all boundary buses have synchrophasor measurements, which extends the applicability of AAM.

3) A new method to automatically identify the warning threshold of area angle is proposed.

4) AAM is verified with both simulated data and synchrophasor measurements for an area in the Western Electricity Coordinating Council (WECC) system.

5) A practical mitigation strategy is proposed to release the stress of the bulk power transfer across the area when area angle exceeds the emergency threshold.

The rest of the paper is organized so that Sections II and III give an overview of AAM and a practical framework of AAM, Section IV demonstrates AAM for an area in WECC, and Section V draws the conclusion.

## II. Overview of Area Angle Monitoring

Two buses are connected by two identical lossless transmission lines in Fig. 1. Assume $\theta_{ab}$ is the angle difference between buses $a$ and $b$, $P_{ab}$ is the power flow from bus $a$ to bus $b$, and $P_{ab,max}$ is the maximum power flow from $a$ to $b$.

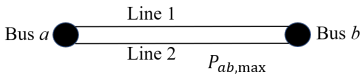


Fig. 1. Monitor stress across two parallel lines with angle difference.

Consider two scenarios:

1. $P_{ab}$ increases.

2. Line 1 is tripped and $P_{ab}$ does not change.

For scenario 1, when $P_{ab}$ increases, $\theta_{ab}$ increases proportionally, indicating the increased stress of power flow. The maximum power flow $P_{ab,max}$ does not change. In scenario 2, line 1 trips, $P_{ab,max}$ decreases and $\theta_{ab}$ increases. Therefore the angle difference $\theta_{ab}$ can indicate the increase of stress caused by either increased power flow or line outage. When a line outage occurs, $P_{ab,max}$ halves and $\theta_{ab}$ doubles. Thresholds for $\theta_{ab}$ can be set up to distinguish outage severity.

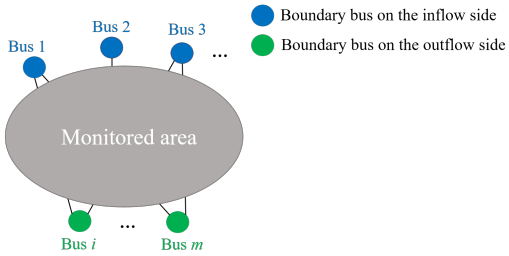


Fig. 2. Schematic diagram of a monitored area.

Area angle [19]–[21] generalizes angle difference between buses to angle difference across an area as in Fig. 2. The stress of bulk power transfer through the area is indicated by a weighted combination of phase angles at the boundary buses of this area as the area angle:

$$\theta_{area} = w_1\theta_1 + w_2\theta_2 + ... + w_m\theta_m \tag{1}$$

where $w_m$ is the weight for bus $m$, $\theta_m$ is the phase angle of bus $m$, and $m$ is the number of boundary buses.

The weights on the boundary buses [19] are calculated as

$$w = (w_1, w_2, ...w_m) = \frac{\sigma_a B_{eq}}{b_{mod}} \tag{2}$$

where $\sigma_a$ is a vector with ones at the positions of the buses at the inflow side of the area and zeros at the positions of the buses at the outflow side, $B_{eq}$ is the equivalent susceptance matrix of the area at the boundary buses, and $b_{mod} = \sigma_a B_{eq} \sigma_a^T$ is the bulk susceptance of the area.

It is approximately the case that the monitored area angle gets larger as the maximum power that could enter the area decreases. This property can be used to set up alarm/warning and emergency thresholds to monitor the area stress [21].

The reason for using the area angle to monitor stress for only one particular pattern of power flow through only one specific area is that if the area angle indicates too much stress, the mitigating action is clearly to reduce that particular power flow through the area [21]. That is, monitoring the area angle for a specific area gives actionable information. Other area angles

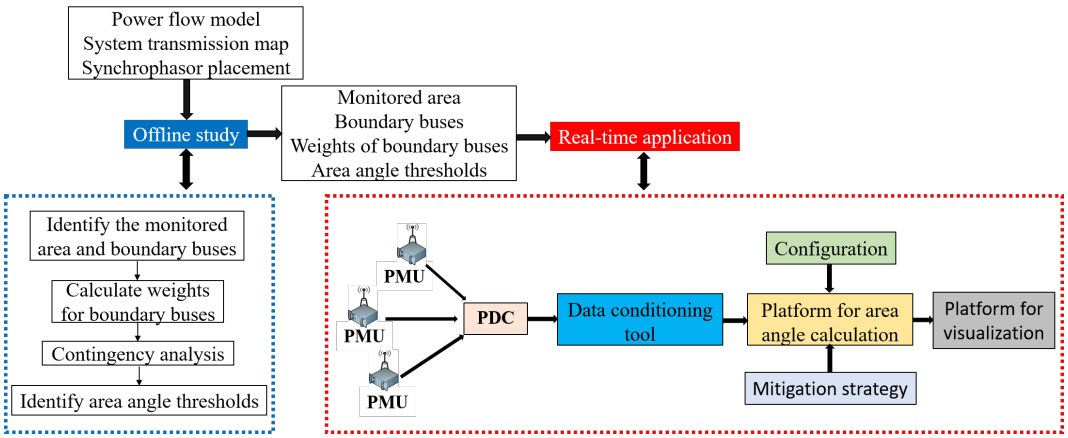


Fig. 3. A practical framework of AAM.

can be set up and monitored for other areas and patterns of stress as needed. In contrast to the area angle, more generic combinations or selections of angle differences can indicate a general stress but are not well associated with specific actions.

Note that an area angle is inherently a difference of angle between two sides of an area. If there are not two sides, then an angle difference between the sides does not make sense and cannot be defined. Area angle can be also defined for some interfaces, if the interface has power flowing in one side and power flowing out another side of the interface.

## III. Framework of Area Angle Monitoring

We propose a practical framework of AAM shown by Fig. 3. It gives the core components (offline study and real-time application) needed for utilities to apply AAM in real-time using synchrophasor measurements.

The offline study provides the monitored area, the boundary buses, weights of boundary buses, and area angle thresholds. They are needed for the calculation of area angle and detection of system status in real-time application. The inputs of the offline study include the power flow model, the system transmission map, and the synchrophasor placement.

The offline study shown in the blue dashed box in Fig. 3 mainly involves 4 steps:

Step 1: Select a monitored area using the system transmission map, the synchrophasor placement and the information contained in the power flow model, and identify the boundary buses of the monitored area that mostly have synchrophasor measurements.

Step 2: Calculate weights for the boundary buses with Kron reduction.

Step 3: Contingency analysis. Calculate the maximum powers that could enter the monitored area and the corresponding area angles under N-1 contingencies. For more details see subsection III-D in [21].

Step 4: Identify area angle thresholds based on the results from Step 3. This will be discussed in subsection III-A.

For real-time application shown in the red dashed box in Fig. 3, synchrophasor measurements are collected in a Phasor Data Concentrator (PDC) from PMUs in substations. Since some low-quality synchrophasor measurements could affect the accuracy of area angle, these data will be first processed by data conditioning tool. Then the processed data are sent to a platform for calculating area angle. The calculation needs a pre-defined configuration, including the boundary buses, weights of boundary buses, and area angle thresholds. Then the results are visualized and shown to system operators. Warning or emergency status will be detected if the area angle exceeds the corresponding threshold. A mitigation strategy will be recommended to reduce the area stress if emergency status is detected. A real-time monitoring platform of AAM is implemented and deployed at BPA, as described in subsection IV-H.

Low-quality synchrophasor measurements include bad data, dropouts, communication issues, time errors etc. There are several ways used in the paper to minimize the impact of low quality data on the accuracy of area angle.

1) Using PMU status flags - The status flag provided along with PMU measurements indicate the quality of the data at the PMU level. PMU status flag can provide the below indicators for each data point.

- Data Invalid
- GPS Out of Synch
- PMU Error
- Sort by Arrival
- Drop Out
- Missing Data
- Data Valid

2) Signal level assessment - Even when PMU status indicates 'Good', further data quality checks are performed at the signal level using range check and stale check. These checks are performed by validating individual signal values and comparing them against their typical ranges. Stale check is used to identify scenarios where data values are constant/stale and do not change at all for a long period of time (e.g. 1 minute and above).

Based on the above two data quality checks, each data point is flagged accordingly. If the data point is not flagged as good, the area angle will not provide a result for that point and suppress any alarms based on low quality synchrophasor data. Data validation is performed as indicated above to ensure that the area angle results are meaningful in all scenarios.

3) Outlier - If an outlier is existing in one or a few phase angles of PMU signals, it may cause the calculated area angle to exceed the area angle thresholds and trigger false detection of warning or emergency status, so a time delay $t_{area}$ is introduced to prevent false detection. This means only if a continuous detection of warning or emergency status for the time period of $t_{area}$, then the detected status will be indicated.

In addition to the above checks, some techniques [22] pioneered a purely data-driven method to improve synchrophasor data quality. These methods apply low-rank matrix factorization techniques to detect and repair low-quality synchrophasor data. They has satisfactory performance under both normal and fault-on operating conditions. They can also be integrated into the proposed framework.

### A. Area Angle Thresholds

Reference [21] defines an emergency threshold of area angle, but the warning threshold is subjective. This paper proposes a general method to identify the warning threshold automatically.

Consider the set of maximum powers that could enter the monitored area without violating line flow limits under N-1 with $n$ line contingencies as $\{P^1_{mod}, ..., P^i_{mod}, ..., P^n_{mod}\}$ sorted into a descending order. $P^1_{mod}$ corresponds to the least severe contingency, $P^i_{mod}$ corresponds to contingency $i$ and $P^n_{mod}$ corresponds to the most severe contingency.

The area is placed in the limit of the maximum power $P^n_{mod}$ corresponding to the most severe contingency $n$, then the area angle $\theta^i_{mod}$ after the contingency of line $i$ is calculated as:

$$\theta^i_{mod} = w_1\theta^i_1 + w_2\theta^i_2 + ... + w_m\theta^i_m \tag{3}$$

where $\theta^i_m$ is the phase angle of boundary bus $m$ under contingency $i$. Doing this calculation for each contingency gives the set of area angles $\{\theta^1_{mod}, ..., \theta^i_{mod}, ..., \theta^n_{mod}\}$.

The standard deviation for three consecutive points in $\{P^1_{mod}, ..., P^i_{mod}, ..., P^n_{mod}\}$ is calculated as

$$\sigma_k = \sigma([P^{k-2}_{mod}, P^{k-1}_{mod}, P^k_{mod}]), \quad 3 \le k \le n \tag{4}$$

starting with $k$=3 and increasing $k$ until $\sigma_k \ge \tau$, where $\tau$ is a constant. Then the warning threshold is

$$\theta^{thr,w}_{mod} = \theta^k_{mod} \tag{5}$$

$\theta^{thr,w}_{mod}$ is the first point at which the maximum powers decrease significantly, indicating a relatively heavy stress inside the monitored area. Any other contingency that causes the area angle to be larger than $\theta^{thr,w}_{mod}$ will give the warning status. Also practically useful is that no action is needed if the area angle is less than $\theta^{thr,w}_{mod}$. Note that other methods such as the first order difference can also be used to identify the warning threshold.

The area angle corresponding to $P^n_{mod}$ is identified as the emergency threshold [21]:

$$\theta^{thr,e}_{mod} = \theta^n_{mod}. \tag{6}$$

$\theta^{thr,e}_{mod}$ corresponds to the largest area stress satisfying the N-1 security criterion. Any multiple contingencies that cause the area angle to be larger than $\theta^{thr,e}_{mod}$ will give emergency status since they correspond to violating the N-1 criterion.

Note that the area angle calculated in real-time does respond to different stresses of power flow through the monitored area caused by different operating conditions. For area angle thresholds, they are identified by considering different stresses reflected by the set of maximum powers $\{P^1_{mod}, ..., P^i_{mod}, ..., P^n_{mod}\}$. For $P^i_{mod}$, it is the maximum power which could enter the monitored area without violating line flow limits after contingency $i$. It is calculated by stressing the monitored area with increased power injections at the boundary buses until any line within the monitored area reaches its line limit. This procedure does consider and quantify the impact of different operating conditions on the stress of power flow through the monitored area. $P^n_{mod}$ is the smallest value in $\{P^1_{mod}, ..., P^i_{mod}, ..., P^n_{mod}\}$, it is the maximum power (corresponding to the largest area stress) that could enter the monitored area without violating N-1 criterion. Therefore the identification area angle thresholds does consider different stresses caused by different operating conditions.

The area angle is aimed at line overloads, which for short lines are usually thermal limits. If, when setting the thresholds, line limits which are proxies for other problems such as stability are used, then the thresholds can also reflect those limits.

### B. Area Angle Thresholds with Angle Compensation

The thresholds of area angle obtained from subsection III-A are based on the power flow model. There may be a mismatch of area angle calculated from the power flow model and real-time monitoring with synchrophasor measurements for normal status. The mismatch is defined as

$$\Delta\theta_{com} = \theta_{ope} - \theta_{mod} \tag{7}$$

where $\theta_{mod}$ is the area angle obtained from the power flow model for normal status and $\theta_{ope}$ is the area angle obtained from real-time operation for normal status. In order to match the normal status from the power flow model to the normal status from real-time monitoring, we select area angles calculated from those PMU datasets whose summation of power flow on the tie lines connected to the boundary buses at the inflow side is close to that calculated from the power flow model (no line outage within the monitored area). This can basically match the operating condition for the monitored area between the power flow model and real-time operation. The average value of area angles from the selected PMU datasets is taken as $\theta_{ope}$.

By compensating the angle thresholds obtained from the power flow model with $\Delta\theta_{com}$, the area angle thresholds for real-time monitoring are calculated:

$$\theta^{thr,w}_{ope} = \theta^{thr,w}_{mod} + \Delta\theta_{com} \tag{8}$$

$$\theta^{thr,e}_{ope} = \theta^{thr,e}_{mod} + \Delta\theta_{com} \tag{9}$$

### C. Detection of Warning and Emergency Status

For real-time monitoring of area angle, when $\theta^{thr,w}_{ope} \le \theta_{area} < \theta^{thr,e}_{ope}$, a warning status is detected and indicated.

When $\theta_{area} \geq \theta_{ope}^{thr,e}$, an emergency status is detected and indicated. Under the emergency status, control actions need to be taken immediately to reduce the stress of bulk power transfer inside the area. As mentioned above, if an outlier is existing in one or a few phase angles of PMU signals, it may cause the calculated area angle to exceed the area angle thresholds and trigger false detection of warning or emergency status. A time delay $t_{area}$ is considered to prevent false detection of warning or emergency status. That is, the detected status will be indicated only if there is continuous detection of warning or emergency status for the time period of $t_{area}$. A longer time delay is more stable in providing a correct alarm, whereas a shorter time delay can give system operators more time to perform a mitigation strategy. We suggest a 5s time delay.

### *D. Mitigation Strategy for Reducing Bulk Power Stress of Monitored Area*

If the area angle exceeds the emergency threshold, indicating that the stress of bulk power across the area violates the N-1 criterion, the stress needs to be mitigated quickly. The area angle has an advantage of a physical interpretation as the angle across the area satisfying Ohm's law [19]. Ohm's law ensures that a mitigation strategy reducing the power flow through the area will reduce the area angle proportionally. Another advantage of real-time AAM is that if operators perform the mitigation, they can quickly see the response of area angle to verify the mitigation.

One simple mitigation strategy is generator ramp up or load shedding on the outflow side of the area. This is equivalent to and can be tested by shedding load on the boundary buses at the outflow side of the area. The reason to use load shedding as the mitigation strategy is because usually there is major generation at the inflow side of the monitored area and major load at the outflow side of the monitored area. The resources to adjust generation at the outflow side are quite limited. Assuming the total amount of load to shed is $L_{total}$, we shed load on each outflow bus proportionally to the magnitude of its weight:

$$L_j = |w_j| L_{total}, \quad 1 \leq j \leq r \tag{10}$$

where $r$ is the number of boundary buses at the outflow side. (Note that the boundary buses on the outflow side have negative weights that sum to $-1$.)

We can set up three stages of load shedding. When the area angle exceeds the emergency threshold, $L_{total}/3$ of load shedding is performed on the outflow side for the first stage, then the system operators can verify the change of area angle immediately. If it still exceeds the emergency threshold, the second stage load shedding $L_{total}/3$ can be performed until the area angle becomes lower than the emergency threshold.

### *E. Estimating Angles on Boundary Buses without Synchrophasors*

For the calculation of area angle, the ideal situation is that all boundary buses are installed with synchrophasors. However, in reality, it is common that not all boundary buses are installed with synchrophasors.

Consider a scenario shown by Fig. 4: buses 1 and 2 are far away from the boundary bus $i$ and they have synchrophasor measurements, and buses 3, 4, 5 without synchrophasor measurements are the neighbors of bus $i$. The phase angle of bus $i$ cannot be estimated using buses 1 and 2 directly.

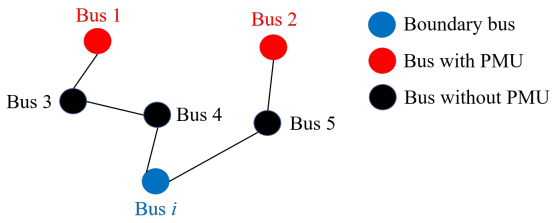


Fig. 4. Estimating phase angle of bus $i$ using PAC.

A practical method to roughly estimate the phase angle of bus $i$ using Phase Angle Compensation (PAC) is proposed as (11).

$$\theta_i = \theta_{j,sm} + \theta_{i,PAC} \tag{11}$$

where $\theta_{j,sm}$ is the phase angle of bus $j$ with synchrophasor measurements ($j$ is 1 or 2 in Fig. 4). The PAC $\theta_{i,PAC}$ of boundary bus $i$ is the angle difference between bus $i$ and bus $j$ calculated from DC power flow in the offline study. Bus $j$ is the bus with synchrophasor measurements closest to bus $i$ in terms of electric distance.

The set of PACs is obtained from offline study and used in real-time, and we prefer to use a constant set of PACs rather than updating it frequently since it involves several steps from the offline study. The case studies in subsection IV-E test the accuracy of PAC for estimating area angle.

Note that if the scenario in Fig. 5 is satisfied, linear state estimation [23] can also be used to estimate the phase angle of boundary bus $i$. In Fig. 5, bus $i$ is a boundary bus without synchrophasor measurements connected by a transmission line to bus 1 with synchrophasor measurements. The phase angle of bus $i$ can be estimated if bus 1 has voltage measurement and a current measurement on the transmission line and the impedance of the transmission line is known.

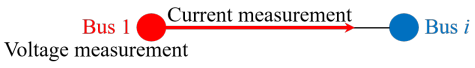


Fig. 5. Linear State Estimation of bus $i$ phase angle using voltage and current PMU measurements at neighboring bus 1.

### *F. Updating Area Angle Thresholds when Topology Changes Significantly*

The area angle thresholds are identified offline and used in real-time. The area angle does respond to different operating conditions, whereas the area angle thresholds do not require very frequent updating. However, they are not updated under contingencies. They only need to be updated when the system

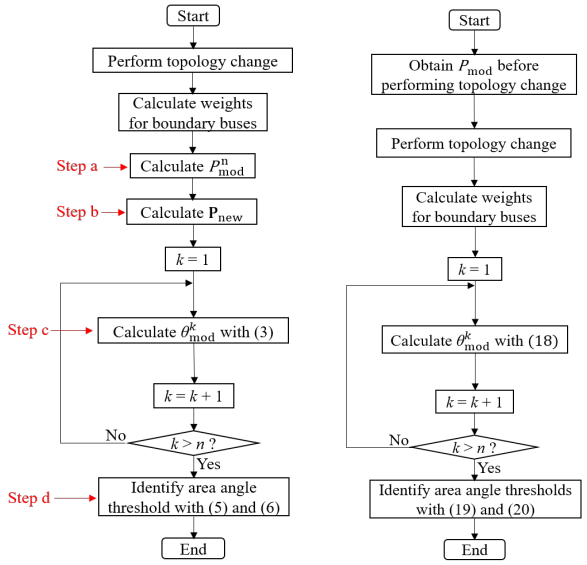


(a) Original method (b) Proposed method

Fig. 6. Methods for updating area angle thresholds under topology change.

topology changes significantly, such as in scheduled maintenance.

*1) Original Method*

Reference [21] does not explicitly present a method to update area angle thresholds, but a similar approach can be summarized by Fig. 6(a). There are 4 important steps:

Step $a$: Calculate the set of maximum powers $\{P^1_{mod}, P^2_{mod}, ..., P^n_{mod}\}$ for all N-1 contingencies sorted into a descending order. Select the maximum power $P^n_{mod}$ with the worst case contingency.

Step $b$: Obtain a new bus injection vector $P_{new}$ by placing the area in the condition of limit of $P^n_{mod}$.

Step $c$: For contingency $k$, calculate the area angle $\theta^k_{mod}$.

Step $d$: Identify area angle thresholds with (5) and (6). Note that (5) is not used by [21].

The area angle for contingency $k$ using the weights before contingency $k$ is calculated as (12):

$$\theta^k_{mod} = w\theta^k_m = \frac{\sigma_a B_{eq}}{b_{mod}}\theta^k_m \tag{12}$$

$$\theta^k_m = e_{ab} \cdot [(B^k)^{-1} P_{new}] \tag{13}$$

where $\theta^k_m$ is the vector of phase angles for the boundary buses, $B^k$ is the susceptance matrix under contingency $k$, $e_{ab}$ is the column vector of length $n$ with ones at the positions for the boundary buses.

*2) Proposed Method*

The original method needs steps a,b,c,d to calculate the area angle for each contingency. Among these, step a is especially complex and it requires the calculation of $\{P^1_{mod}, P^2_{mod}, ..., P^n_{mod}\}$. In order to avoid this calculation, we propose the simplified approximate method of Fig. 6 (b).

If the topology change caused by contingency $k$ is considered in the calculation of weights, the calculated area angle using the updated weights is indicated by $\theta^{[k]}_{mod}$, where

$$\theta^{[k]}_{mod} = \frac{\sigma_a B^k_{eq}}{b^k_{mod}}\theta^k_m \tag{14}$$

$B^k_{eq}$ is the equivalent susceptance matrix of the boundary buses considering contingency $k$, and $b^k_{mod}$ is the bulk susceptance of the area considering contingency $k$.

Apply Ohm's law to the area angle at the maximum power transfer of the base case to get

$$P_{mod} = b_{mod}\theta_{mod} \tag{15}$$

where $P_{mod}$ is the base case maximum power through the area without violating the line flow limits, and $\theta_{mod}$ is the corresponding area angle with $P_{mod}$ through the area.

Also, considering the maximum power transfer when contingency $k$ occurs, we have

$$P^k_{mod} = b^k_{mod}\theta^{[k]}_{mod} \tag{16}$$

where $P^k_{mod}$ is the maximum power through the area considering contingency $k$, and $\theta^{[k]}_{mod}$ is the corresponding area angle with $P^k_{mod}$ through the area.

The results from section 4.4 in [26] show that $\theta^{[k]}_{mod} \approx \theta^k_{mod}$. Then we can have:

$$P^k_{mod} = b^k_{mod}\theta^k_{mod} \tag{17}$$

Sometimes there are no parallel paths outside the area for power transfer from the inflow side to the outflow side of the area. The area is a cutset area [19], [20]. Then when a non-islanding contingency $k$ occurs, the generation stays the same and $P^k_{mod} = P_{mod}$. Moreover, there is a good approximation when the parallel paths outside the area have high impedance. In this case, when a non-islanding contingency $k$ occurs, $P^k_{mod} \approx P_{mod}$ [26], [27]. So we have:

$$\theta^k_{mod} = \frac{P^k_{mod}}{b^k_{mod}} \approx \frac{P_{mod}}{b^k_{mod}} \tag{18}$$

This approximation, but applied to the monitored area angle instead of the threshold angle, is also used and discussed by eqn. (13) in [27].

Instead of using (5) and (6), we propose the approximate emergency threshold $\hat{\theta}^{thr,e}_{mod}$ and warning threshold $\hat{\theta}^{thr,w}_{mod}$ as

$$\hat{\theta}^{thr,e}_{mod} = \max\{\theta^1_{mod}, \theta^2_{mod}, ..., \theta^n_{mod}\} \tag{19}$$

$$\hat{\theta}^{thr,w}_{mod} = \frac{1}{2}\left[\hat{\theta}^{thr,e}_{mod} + \min\{\theta^1_{mod}, ..., \theta^n_{mod}\}\right] \tag{20}$$

The warning threshold (20) is the average value of the minimum and maximum values of $\{\theta^1_{mod}, \theta^2_{mod}, ..., \theta^n_{mod}\}$. Since the emergency threshold is used to detect more severe events, its approximation (19) is acceptable only if it is sufficiently accurate. The case study in subsection IV-F compares the approximate and original area angle thresholds.

### G. Discussion on Implementing AAM for an Utility System

There are some difficulties to implement the framework shown in Fig. 3 for an utility system. Firstly, it is not easy to select a monitored area. The area requires a particular pattern of power flow through it that stresses the area to be identified, and this requires engineers to be familiar with the operation of the target utility system. Secondly, after the monitored area is selected, the set of boundary buses need to be identified. It means that the area should be connected (no islands) and the

area has to be completely separable by clear boundaries from the other buses of the remaining system. Area selection is not an automatic process now and requires much time and effort. Thirdly, some identified boundary buses are not installed with synchrophasor measurements, which has been discussed in subsection III-E. Fourthly, some low-quality synchrophasor measurements may affect the accuracy of area angle, which has been discussed in Section III.

## IV. Case Studies

### A. Model and Parameter Preparation

The offline study in Fig. 3 uses the power flow model for the 2020 heavy summer case of the WECC system provided by BPA.

PMUs are mainly deployed for high-voltage power transmission. For a reduced power flow model with high-voltage level, it is relatively easy to select a monitored area with a large coverage of synchrophasor measurements on the boundary buses. However, the model we have is a detailed model, and under this circumstance, static network reduction is needed.

A reduced/equivalent model ($\geq$ 230kV) is obtained using the modified Ward reduction [24]. Note that Kron reduction is a standard tool to obtain a "network-reduced" or "Ward-equivalent" model for power flow studies [25]. The main difference between the Kron/Ward reduction and the modified Ward reduction is that all generators in the original model are retained integrally in the reduced model with the modified Ward reduction. Reference [24] verifies the accuracy of the modified Ward reduction by comparing the power flows of the original and reduced models. The original and reduced models are compared in Table I.

TABLE I. Comparison of Models

| | Original Model | Reduced Model |
|---|---|---|
| Number of Buses | 20507 | 3101 |
| Number of Generators | 4019 | 4014 |
| Number of Lines | 26395 | 8000 |

The parameters chosen are $\tau = 0.5$ p.u. and $t_{area} = 5$ s. The offline study of AAM in Fig. 3 is implemented with MATLAB R2019a.

### B. Monitored Area and Area Angle Thresholds

A monitored area is selected inside the reduced model of WECC. The monitored area roughly covers Oregon state which is in BPA's territory and contains 176 transmission lines and 106 buses. The bulk power transfer of interest is from north (inflow side) to south (outflow side). There are 14 boundary buses; 7 of them are on the inflow side and 7 are on the outflow side. The area angle weights of buses 1–7 on the inflow side are [0.1271, 0.5303, 0.2616, 0.0396, 0.0385, 0.0005, 0.0023], and the weights of buses 8–14 on the outflow side are [–0.1269, –0.0958, –0.0017, –0.1615, –0.2979, –0.2766, –0.0395].

*1) Maximum Powers and Area Angles under N-1 Contingencies*

To set the emergency threshold, we need to examine the worst case maximum powers that could enter the monitored area under N-1 line contingencies. The maximum powers that could enter the monitored area and area angles corresponding to the non-islanding N-1 contingencies are shown by Fig. 7 (a). Basically the area angle increases as the maximum power decreases [21]. This verifies that area angle can distinguish the stress of bulk power transfer caused by different contingencies. Fig. 7 (a) is used to set the emergency threshold.

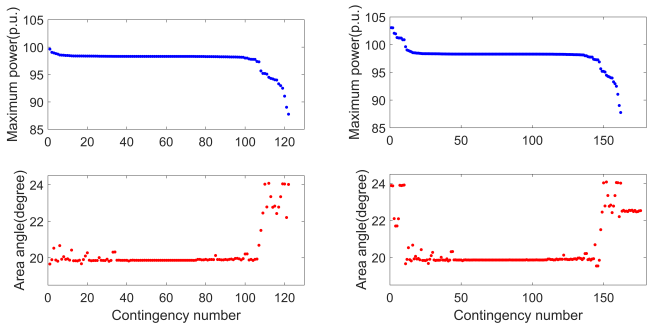


(a) N-1 contingencies; equivalenced lines excluded

(b) N-1 contingencies; all lines in reduced model

Fig. 7. Maximum powers and area angles.

Note that Fig. 7 (a) excludes lines that are equivalenced in the reduced model; that is, we only apply the N-1 criterion to lines within the monitored area in the reduced model that also appear in the original model. The reason is that removing an equivalenced line in the reduced model has an effect that is unrelated to the effect of removing a line in the original model, so that applying the N-1 criterion with the equivalenced lines does not correctly reflect the N-1 criterion applied to the real system. We can see the effect of applying the N-1 to all the lines within the monitored area of the reduced system, including the 54 equivalent lines (176 lines inside the area), in Fig. 7(b), as additional more extreme outliers. (Of course, one way to prevent problems with equivalenced lines is to avoid system reduction, but that entails a larger system model.)

We check that the 6581 lines of the detailed model eliminated in the system reduction do not significantly affect the area angle by removing each of those lines in the detailed model, obtaining a new reduced model with each of those lines in the detailed model removed, and recalculating the area angle with the system placed in the condition of limit of $P^n_{mod}$. The recalculated area angles are within 0.4 degree of the baseline of area angles in Fig. 7(a), indicating that the N-1 contingencies of the lines eliminated in the reduction have little effect on the stress inside the monitored area.

*2) Area Angle Thresholds*

The maximum power that could enter the monitored area and its corresponding area angle under N-1 contingency is used to identify area angle thresholds. The standard deviation using (4) is calculated and shown in Fig. 8.

From Fig. 8, we can see that the first data point satisfying $\sigma_i \geq \tau$ is $i$=108 and its corresponding area angle is 21.49 degree, which is selected as the warning threshold. The area angle obtained from (6) is 24.07 degree, which is the emergency threshold.

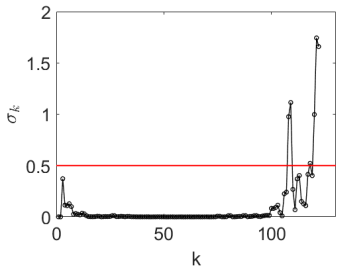


Fig. 8. Standard deviation of maximum power under N-1 contingency.

Note that $\tau$ is set to 0.5 p.u. for this area. There is no analytical method to determine $\tau$ right now. One way to determine it is to check the baseline of maximum powers and use a percentage to calculate $\tau$. In our case, the baseline of maximum power seen from Fig. 7(a) is around 98 p.u. We use 5% of 98 p.u., i.e. 0.5 p.u as $\tau$. It is a constant for one monitored area. However, since the curve shape of maximum power and its baseline could vary for different areas, we do not suggest using one $\tau$ for different areas. For a new monitored area, it would be better to first plot the curve of maximum power and then set up $\tau$ accordingly.

The value of $\Delta\theta_{com}$ is calculated as -0.7 degree, and is used to adjust the warning and emergency thresholds for real-time monitoring with (8) and (9) as shown in Table II. In the following sections, $\theta_{ope}^{thr,w}$ and $\theta_{ope}^{thr,e}$ are used for the warning and emergency thresholds.

TABLE II. Area Angle Thresholds

| Threshold | Value of Threshold (Degree) |
|---|---|
| $(\theta_{mod}^{thr,w}, \theta_{mod}^{thr,e})$ | (21.49, 24.07) |
| $(\theta_{ope}^{thr,w}, \theta_{ope}^{thr,e})$ | (20.79, 23.37) |

### C. Verification of Area Angle With Simulated Data

This subsection is used to verify that area angle does respond to the change of operating conditions which stress the monitored area. 1) is used to verify that area angle does respond to the change of operating condition caused by the contingencies outside the monitored area. It is also verified area angle is related to system load level for the same contingency. Therefore light, medium, and heavy loadings are considered. The difference of active power between heavy and medium loadings is 1 000 MW, and the difference of active power between medium and light loadings is around 23 000 MW. They are used to study the impact of small change and big change of loadings on area angle, respectively. 2) is used to verify that area angle does respond to contingencies happening within the monitored area.

GE Positive Sequence Load Flow Software V21.5 is used to generate the simulated data. In order to capture the variation of area angle, dynamic simulation is performed. Phase angles obtained from dynamic simulation can be used as fictitious synchrophasor measurements. The method in subsection III-E is used.

*1) Verification of Area Angle with Generator Trip*

Contingency 1: Trip of one generator (around 1400 MW output) in the southern part of the outflow side of the monitored area at 60 s.

Contingency 2: Trip of two generators (around 2800 MW output) in the southern part of the outflow side of the monitored area at 60 s.

These contingencies are outside the area and they reduce the generation on the outflow side of the monitored area, and thus increases the bulk power transfer through the monitored area.

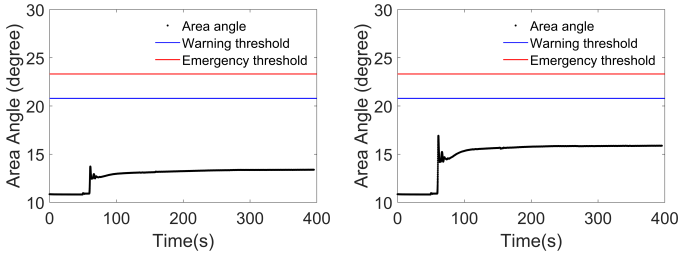


(a) Contingency 1 (b) Contingency 2

Fig. 9. Area angle under generator trip for light loading.

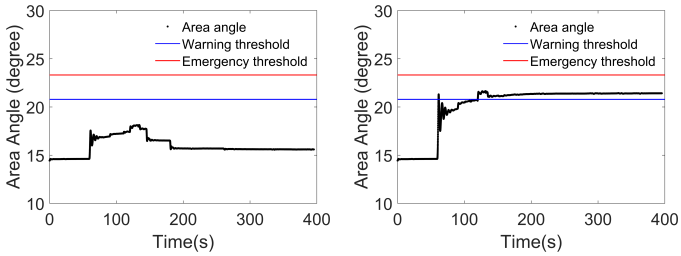


(a) Contingency 1 (b) Contingency 2

Fig. 10. Area angle under generator trip for medium loading.

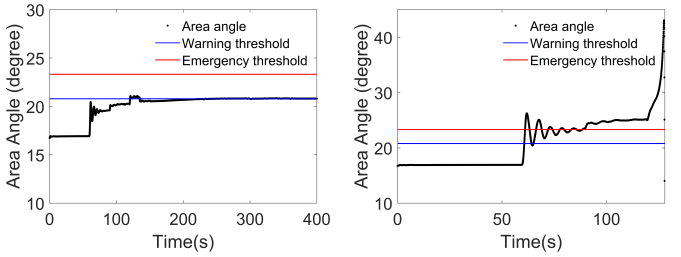


(a) Contingency 1 (b) Contingency 2

Fig. 11. Area angle under generator trip for heavy loading.

From Fig. 9, we can see that the area angle increases after the contingency occurs, indicating the increased stress of bulk power transfer through the area. But the contingencies do not cause area angle to exceed any threshold. By comparing Fig. 9 (a) with Fig. 9 (b), we can see that the area angle increases more obviously for Contingency 2 when compared with Contingency 1, it is because the increased bulk power through the area is larger for Contingency 2.

From Fig. 10, we can see that the area angle increases after the contingency occurs. For Contingency 2, the area angle exceeds the warning threshold. By comparing area angles during steady-state periods (pre-contingency and post-contingency) between Fig. 10 (a) and Fig. 9 (a), Fig. 10 (b) and Fig. 9 (b), we can see that area angle increases for the same contingency with different loading levels, this is caused by the increased power through the area as the system load level increases.

From Fig. 11, we can see that Contingency 1 makes the area angle exceed the warning threshold and Contingency 2 makes the area angle exceed the emergency threshold. Warning status and emergency status will be indicated for Contingency 1 and Contingency 2, respectively. Note that the system goes unstable around 120 s for Contingency 2.

*2) Verification of Area Angle with Line Outage*

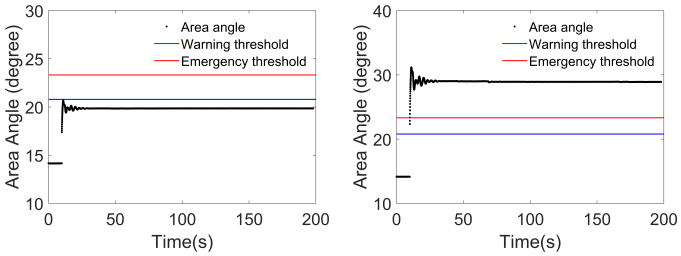


(a) Contingency 3 (b) Contingency 4

Fig. 12. Area angle under line outage for medium loading.

Contingency 3: Trip of one 500 kV line at 10 s.

Contingency 4: Trip of three 500 kV lines at 10 s.

These contingencies are inside the monitored area and they reduce the capability of bulk power transfer inside the monitored area and thus increase the stress. The contingencies are simulated under medium loading.

The area angle in Fig. 12 (a) increases after this contingency occurs but it does not exceed any threshold. Fig. 12 (b) represents a more severe contingency and the area angle exceeds the emergency threshold. Emergency status will be indicated for Contingency 4.

### *D. Verification of Area Angle with Synchrophasor Measurements*

Two sets of recorded synchrophasor measurements from real contingencies are used here. These contingencies happened inside the monitored area.

Contingency 5: Trip of one 500 kV line.

Contingency 6: Trip of two 500 kV lines. The time interval between the two line outages is around 100 s.

From Fig. 13 (a), we can see that the area angle varies for the whole time period but does not exceed any threshold.

From Fig. 13 (b), we can see that the area angle increases significantly after the first line outage and continues increasing after the second line outage. It is a N-2 contingency. It causes area angle to exceed the warning threshold for more than 5 s. The warning status will be indicated.

We consider two other contingencies.

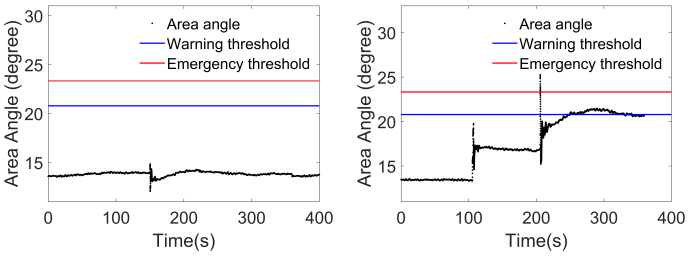


(a) Contingency 5 (b) Contingency 6

Fig. 13. Area angle with synchrophasor measurements for contingencies 5 and 6.

Contingency 7: Trip of one 500 kV line.

Contingency 8: Trip of one 230 kV line.

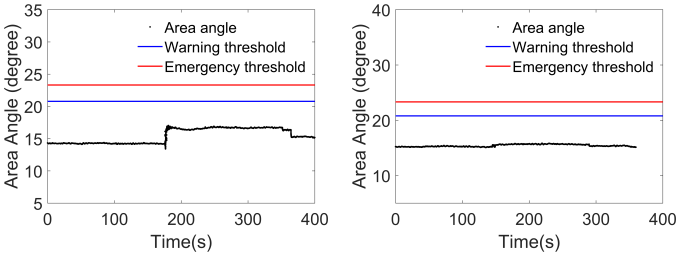


(a) Contingency 7 (b) Contingency 8

Fig. 14. Area angle with synchrophasor measurements for contingencies 7 and 8.

From Fig. 14 (a) and Fig. 14 (b), we can see that they do not cause area angle to exceed any threshold.

From Fig. 13 and Fig. 14, we can also know that area angle thresholds are quite reliable since those N-1 contingencies happening within the monitored area will not cause the area angle to exceed area angle thresholds.

### *E. Influence of PACs on the Accuracy of Area Angle*

For the boundary buses without synchrophasor measurements, the PACs are calculated and shown in Table. III.

TABLE III. PACs for Some Boundary Buses without Synchrophasors

| Boundary Bus Number | PAC (Degree) | Weight |
|---|---|---|
| 4 | -1.8633 | 0.0396 |
| 5 | -3.1933 | 0.0385 |
| 6 | -1.0322 | 0.005 |
| 7 | 2.7367 | 0.0023 |
| 8 | 0.0968 | -0.1269 |
| 9 | -8.7963 | -0.0958 |
| 10 | -9.5810 | -0.0017 |
| 14 | -3.9630 | -0.0395 |

The influence of PACs on the accuracy of area angle is investigated with Contingency 1 under heavy loading.

In Fig. 15 (a), the curve marked by “PMUs” assumes that all boundary buses are installed with synchrophasor measurements. The curve marked by “PMUs and PAC” uses the Phase Angle Compensation method in subsection III-E. From Fig. 15 (b), we can see that the largest mismatch is around 0.06

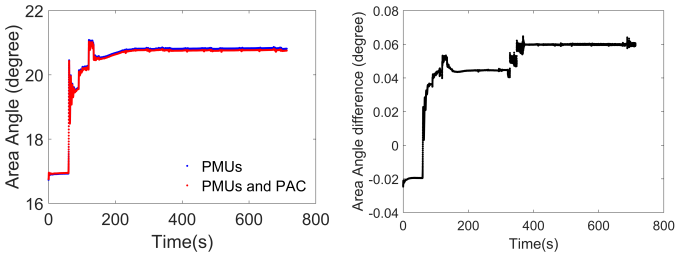


(a) Area angle comparison (b) Area angle difference

Fig. 15. Influence of PACs on area angle for Contingency 1.

degree. It suggests that the PAC method is accurate enough to calculate area angle. We can see that the weights for those boundary buses without synchrophasor measurements are quite small and the absolute values of PACs are not large, thus the influence on the accuracy of area angle is very small.

The PAC values obtained from a power flow model could vary with system operating condition. We investigate the impact of using different sets of PAC values on the area angle. Different sets of PAC values obtained from light, medium and heavy loading conditions with the reduced model are used with Contingency 1. The heavy and medium loadings are used to study the influence of small variation of load level on PAC values and area angle. The medium and light loadings are used to study the influence of large variation of load level on PAC values thus area angle.

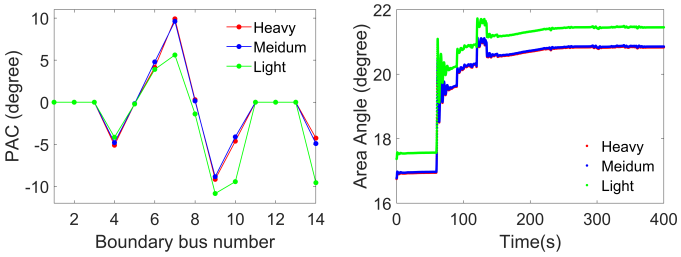


(a) PAC comparison (b) Area angle comparison

Fig. 16. Influence of different sets of PACs on area angle.

From Fig. 16, the area angle curves are almost overlapped for the sets of PACs obtained from the medium and heavy loadings. However, the area angle difference is relatively large for using two sets of PACs obtained from the medium and light loadings. This is caused by the large difference of loading level between medium and light loading conditions, which is approximately 12% of the original system loading level. The larger the loading difference, the larger the difference of the PACs and thus the area angle. However, in real-time operations, such a significant change of loading is rare.

In summary, the accuracy for calculating area angle with a set of PACs is quite high if the weights for those boundary buses without synchrophasor measurements are small and there is no significant change of loading in the system. In extreme cases, if both conditions are not satisfied, the error for the estimation of area angle will become large.

### F. Updating Thresholds Under Significant Topology Change

Consider the maintenance of two lines inside the monitored area, the updated warning and emergency thresholds using two methods are given in Table IV. The results using the original method are benchmarks.

TABLE IV. Area Angle Thresholds

| | Warning Threshold | Emergency Threshold |
|---|---|---|
| Original Method | $\theta_{mod}^{thr,w}$=22.08 | $\theta_{mod}^{thr,e}$=26.75 |
| Proposed Method | $\hat{\theta}_{mod}^{thr,w}$=23.44 | $\hat{\theta}_{mod}^{thr,e}$=26.88 |

From Table IV, the mismatch of $\theta_{mod}^{thr,w}$ between two methods is 6.16%, which is not small. The mismatch of $\theta_{mod}^{thr,e}$ between two methods is 0.49%, which is very small. Since mitigation strategies are needed if the area angle exceeds the emergency threshold, we are more concerned about the accuracy of emergency threshold. Thus the accuracy of the proposed method for updating area angle thresholds is acceptable.

### G. Mitigation Strategy for Reducing the Bulk Power Stress

Contingencies 9, 10, and 11 are used to verify the proposed mitigation strategy in subsection III-D. Each contingency has three stages. The first stage is the normal state before the contingency. The second stage is immediately after the contingency. The third stage is after the mitigation of load shedding on the buses of outflow side.

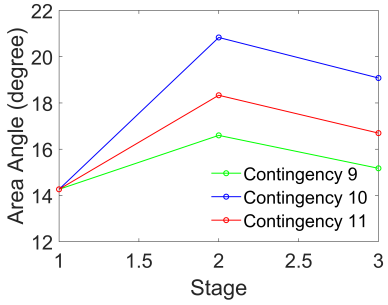


Fig. 17. Reduce area angle for three contingencies.

From Fig. 17, we can see that the area angle increases at stage 2 compared with that of stage 1 and then decreases at stage 3 after performing load shedding compared with that of stage 2 for each contingency. This shows the proposed mitigation strategy is working to reduce the bulk power stress.

### H. Real-Time Application Platform of AAM

We develop a platform for real-time application of AAM as shown by Fig. 18. Synchrophasor measurements collected by PDC are sent out to Data Quality Management Platform (DataNXT) for data conditioning. Then the processed data are sent out to Real Time Dynamics Monitoring System (RTDMS) Server through the C37.118 data stream protocol. The area angle is calculated in the RTDMS Server. The area angle and area angle thresholds are visualized in the RTDMS Client in real-time.

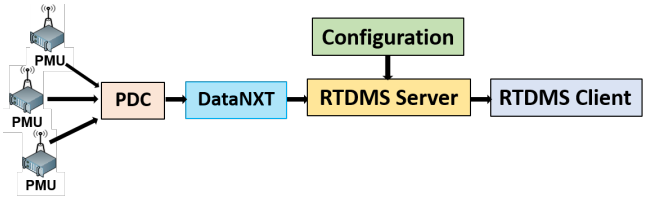


Fig. 18. Platform of real-time application of AAM.

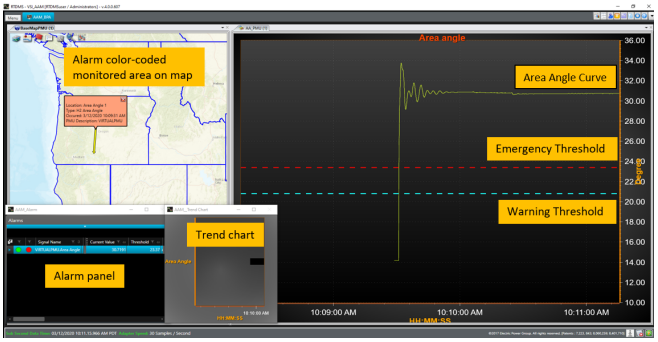


Fig. 19. Visualization of area angle in real-time.

This platform is deployed in BPA. It is running in their laboratory with live stream data from synchrophasor measurements. BPA has also tested it using simulated data and recorded synchrophasor measurements for historical events.

For example, the area angle can be seen in real-time responding to Contingency 4 under medium loading in Fig. 19. The emergency status is reported with red in the "Alarm Panel" after the area angle exceeds the threshold. The mitigation strategy will be implemented into the platform in future work.

## V. Conclusion

This paper develops and applies a practical framework of Area Angle Monitoring (AAM) to monitor the stress of bulk power transfer across an area in real-time using synchrophasor measurements. The framework addresses several challenges for implementing AAM. Methods are proposed to handle incomplete synchrophasor measurements at the boundary of the area, identify the warning threshold of area angle, and quickly update area angle thresholds under significant topology change. A mitigation strategy to relieve the stress of bulk power through the monitored area is suggested. Case studies and a utility deployment for an area demonstrate AAM with both simulated data and recorded and live-stream synchrophasor measurements. The performance of the proposed methods are studied and the proposed mitigation strategy is tested. The innovations and testing of AAM position it as a practical tool for monitoring area stress and suggesting mitigation actions to the operators when thresholds are exceeded.

## References

[1] L. Zhang, H. Chen, Q. Wang, N. Nayak, Y. Gong, A. Bose, "A novel online substation instrument transformer health monitoring system using synchrophasor data," *IEEE Trans. Power Del.*, vol. 34, no. 4, pp. 1451-1459, Aug. 2019.

[2] W. Ju, N. Nayak, et al, "Indices for automated identification of questionable generator models using synchrophasors," *IEEE Power and Energy Society General Meeting*, Montreal, Canada, Aug. 2020.

[3] Y. Zhang, M. E. Raoufat, K. Tomsovic, and S. M. Djouadi, "Set theory-based safety supervisory control for wind turbines to ensure adequate frequency response," *IEEE Trans. Power Syst.*, vol. 34, no. 1, pp. 680-692, Jan. 2019.

[4] R. W. Cummings, in *Predicting Cascading Failures, Presentation at NSF/EPRI Workshop on Understanding and Preventing Cascading Failures in Power Syst.*, Westminster, CO, USA, Oct. 2005.

[5] V. Venkatasubramanian, Y. X. Yue, G. Liu, et al, "Wide-area monitoring and control algorithms for large power systems using synchrophasors," *IEEE Power Syst. Conf. and Exposition*, Seattle, WA, USA, Mar. 2019.

[6] NERC (North American Electric Reliability Council), "Phase angle monitoring: industry experience following the 2011 pacific southwest outage recommendation 27," Jun. 2016.

[7] U.S.-Canada Power System Outage Task Force, "Final report on the August 14, 2003 blackout in the United States and Canada: Causes and Recommendations," Apr. 2004.

[8] NERC (North American Electric Reliability Council), 1996 system disturbances, 2002.

[9] Arizona-Southern California Outages on September 8, 2011: Causes and Recommendations, Federal Energy Regulatory Commission and the North American Electric Reliability Corporation, April 2012.

[10] W. Ju, K. Sun, and R. Yao, "Simulation of cascading outages considering frequency using a dynamic power flow model," *IEEE Access*, vol. 6, No. 1, pp. 37784-37795, 2018.

[11] U. Nakarmi, M. Rahnamay-Naeini, M. J. Hossain, et al, "Interaction graphs for reliability analysis of power grids: A Survey," arXiv:1911.00475v1, Nov. 2019.

[12] W. Ju, K. Sun, and J. Qi, "Multi-layer interaction graph for analysis and mitigation of cascading outages," *IEEE Journal on Emerging and Selected Topics in Circuits and Systems.*, vol. 7, No. 2, pp. 239-249, Jun. 2017.

[13] C. Chen, W. Ju, K. Sun, S. Ma, "Mitigation of cascading outages using a dynamic interaction graph-based optimal power flow model," *IEEE Access*,vol. 7, pp. 168636-168648, 2019.

[14] J. Qi, W. Ju, and K. Sun, "Estimating the propagation of interdependent cascading outages with multi-type branching processes," *IEEE Trans. Power Systems.*, vol. 32, No. 2, pp. 1212-1223, Mar. 2017.

[15] D. Gan, X. Luo, D. V. Bourcier, R. J. Thomas, "Min-max transfer capability of transmission interfaces," *Int. J. Elect. Power Energy Syst.*, vol. 25, no. 5, pp. 347-353, 2003.

[16] Y. V. Makarov, P. Du, S. Lu, T. B. Nguyen, X. Guo, *Wide Area Power System Security Region PNNL-19063*, Richland, WA USA:Pacific Northwest National Lab., 2009.

[17] F. Capitanescu, T. V. Cutsem, "Evaluating bounds on voltage and thermal security margins under power transfer uncertainty," *Proc. PSCC Conf.*, Jun. 2002.

[18] Simultaneous Transfer Capability: Direction for Software Development, Electric Power Research Institute Report EL-7351 Project 3140-1, 1991.

[19] I. Dobson, "Voltages across an area of a network," *IEEE Trans. Power Syst.*, vol. 27, no. 2, pp. 993-1002, May 2012.

[20] I. Dobson, M. Parashar, "A cutset area concept for phasor monitoring," *IEEE Power and Energy Society General Meeting*, Minneapolis, MN USA, Jul. 2010.

[21] A. Darvishi, I. Dobson, "Threshold-based monitoring of multiple outages with PMU measurements of area angle," *IEEE Trans. Power Syst.*, vol. 31, no. 3, pp. 2116-2124, May. 2016.

[22] M. W, L. Xie, "Online detection of low-quality synchrophasor measurements: a data-driven approach," *IEEE Trans. Power Syst*, vol. 32, no. 4, pp. 2817-2827, Jul. 2017.

[23] L. Zhang, A. Bose, A. Jampala, et al, "Design, testing, and implementation of a linear state estimator in a real power system," *IEEE Trans. Smart Grid*, vol. 8, no. 4, pp. 1782-1789, Jul. 2017.

[24] D. Shi, D. L. Shawhan, N. Li, et al, "Optimal generation investment planning: Pt. 1: network equivalents," *North American Power Symposium*, Aug. 2012.

[25] F. Dorfler, F. Bullo, "Kron reduction of graphs with applications to electrical network," *IEEE Trans. Circuits and Systems-I*, vol. 60, no. 1, pp. 150-163, Jan. 2013.

[26] A. Darvishi, "Monitoring of single and multiple line outages with synchrophasors in areas of the power system," PhD. thesis, Iowa State University, Ames, IA, 2015.

[27] A. Darvishi, I. Dobson, "Synchrophasor monitoring of single line outages via area angle and susceptance," *North American Power Symposium*, Pullman WA USA, Sept. 2014.

**Wenyun Ju (S'14-M'18)** received the B.Sc. degree in electrical engineering and automation from Sichuan University, Chengdu, China in 2010, and the M.Sc. degree in electrical and electronic engineering from Huazhong University of Science and Technology, Wuhan, China in 2013, and his Ph.D. degree in electrical engineering from the University of Tennessee, Knoxville, TN, USA in 2018. He is currently a Power System Engineer with Electric Power Group, Pasadena, CA, USA.

**Ian Dobson (F'06)** received the B.A. degree in mathematics from Cambridge University, U.K., and the Ph.D. degree in electrical engineering from Cornell University, Ithaca, NY, USA. He previously worked as an operations analyst in British industry and as a professor at the University of Wisconsin-Madison, USA He is currently Sandbulte Professor of Engineering at Iowa State University, Ames, IA, USA.

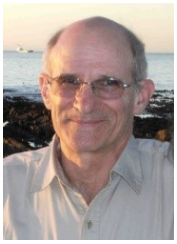

**Kenneth Martin (F'08)** has over 40 years experience in the electric utility industry, first at the Bonneville Power Administration (BPA) in communication, precise timing, instrumentation, and testing. He started working with synchrophasor measurement with the original PMUs in 1987 and conducted the first PMU tests. He developed the phasor measurement system at BPA, including building the first phasor data concentrator, and supported similar developments at many utilities. He chaired the development of the IEEE C37.118 Synchrophasor Standards from the 2005 original, through the 2014 amendment. He was a Lead for the IEC 61850, part 90-5 and is the Convener for 60255-118-1 developing the joint IEC-IEEE measurement standard. He is currently a Principal Engineer with the Electric Power Group (EPG).

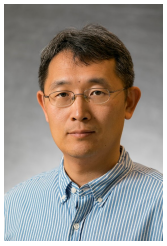

**Kai Sun (M'06-SM'13)** received the B.S. degree in automation in 1999 and the Ph.D. degree in control science and engineering in 2004 both from Tsinghua University, Beijing, China. He is an associate professor at the Department of EECS, University of Tennessee, Knoxville, USA. He was a project manager in grid operations and planning at the EPRI, Palo Alto, CA from 2007 to 2012. Dr. Sun is an associate editor with IEEE Transactions on Power Systems, IEEE Transactions on Smart Grid, IEEE Access and IEEE Open Access Journal of Power and Energy.

**Neeraj Nayak (M'13)** received the B.E. degree in electrical engineering from the Sardar Patel College of Engineering (SPCE), Mumbai, India, in 2012, and the M.S. in electrical engineering from the University of Southern California, California, USA, in 2014. He is currently a Senior Power Systems Engineer with Electric Power Group. His research interests include synchrophasor data analysis, power system oscillation analysis, generator model validation and calibration, synchrophasor based Real-time Contingency Analysis etc.

**Iknoor Singh (M'12)** received his M.Sc. degree from Arizona State University. He is currently a Senior Power Systems Engineer with Electric Power Group and is involved in research and development of synchrophasor applications, such as oscillation source location identification, voltage stability monitoring, phasor simulator for operator training etc. He has also performed analytical studies for establishing alarm thresholds and various event analysis based upon synchrophasor data. Previously, he worked as a power plant layout engineer at Siemens, India.

**Horacio Silva-Saravia (S'10-M'19)** received his B.Sc. and M.Sc. degrees from the Federico Santa Maria Technical University, Chile in 2014, and his Ph.D degree in electrical engineering from the University of Tennessee, Knoxville, TN, USA in 2019. His research area includes power system dynamics, stability and control of renewable energy generation, and PMU applications. He currently works at Electric Power Group in research and development related to synchrophasor technology applications for oscillation detection, oscillation monitoring and linear state estimation.

**Anthony Faris** received his B.Sc. degree from the University of Portland in 2004, and his M.Sc. degree from the University of Washington in 2006. He has worked at Bonneville Power Administration (BPA) since 2004, and is presently leading RD work in Synchrophasor technology, including application development, PMU testing, and Synchrophasor data analysis.

**Lin Zhang (SM'18)** received the B.Eng. degree from Huazhong University of Science and Technology, Wuhan, China, in 2006, M.S from Wuhan University, Wuhan, China in 2008 and Ph.D from Washington State University, Pullman, USA, in 2014. He is currently a senior system performance analysis engineer at American Electric Power.

**Yajun Wang (S'17-M'19)** received the B.Sc. and M.Sc. degrees from the School of Electrical Engineering, Wuhan University, Wuhan, China, in 2012 and 2014, respectively, and the Ph.D. degree in electrical engineering from the University of Tennessee, Knoxville, TN, USA, in 2019. She is currently working with Dominion Energy Virginia, Richmond, VA, USA, as a Senior Power System Engineer. Her research interests are big data analytics, power system stability and control, system restoration, energy storage systems, electric vehicles, and DER integration.